JACS
JOURNAL OF THE AMERICAN CHEMICAL SOCIETY

Communication

pubs.acs.org/JACS

Creating Protein-Imprinted Self-Assembled Monolayers with Multiple Binding Sites and Biocompatible Imprinted Cavities

Xianfeng Zhang, Xuezhong Du,* Xuan Huang, and Zhongpeng Lv

Key Laboratory of Mesoscopic Chemistry (Ministry of Education), State Key Laboratory of Coordination Chemistry, and School of Chemistry and Chemical Engineering, Nanjing University, Nanjing 210093, People's Republic of China

Supporting Information

ABSTRACT: Imprinted monolayers have several advantages over bulk imprinted polymers such as excellent mass transfer of molecules into and out of imprinted sites and transduction of binding signals detected in real time. Protein-imprinted self-assembled monolayers (SAMs) were created with multiple binding sites and biocompatible imprinted cavities from functional thiols and novel disulfide compounds containing an oligoethylene glycol (OEG) terminal moiety and two amide groups incorporated in the chain (DHAP) in a biologically benign solution. DHAP played an important role in the formation of multiple binding sites and biocompatible cavities in addition to resisting nonspecific protein binding. The created protein-imprinted SAMs exhibited the excellent ability of specific binding of target proteins determined by multiple binding sites and imprinted cavities. The strategy generates tailor-made monolayer surfaces with specific protein binding and opens the possibility of controlled assembly of intellectual biomaterials and preparation of biosensors.

Molecular imprinting allows creation of artificial recognition sites in synthetic polymers and has received much attention in the past four decades.[1] Molecularly imprinted polymers have considerable potential for applications in the areas of clinic analysis, medical diagnostics, environmental monitoring, and catalysis.[2] While successful for small-template molecules, the molecular imprinting of proteins faces several problems related to their size, structural complexity, conformational flexibility, and compatibility with solvents.[3] These primarily include reduced mass transfer and permanent retention of protein templates in polymer matrices and restricted selection of aqueous media.[3c,e] The use of water as solvent provides a biologically benign environment for proteins although water can reduce hydrogen bonding and electrostatic interactions between the template molecules and functional monomers. Highly desirable for economical, stable, and recyclable synthetic biological materials, protein imprinting as synthetic antibody mimics, exhibiting excellent chemical, mechanical, and thermal stability, could be substituted for expensive biological antibodies used in isolation and extraction of proteins and biosensing. Imprinting of proteins represents one of the most challenging tasks.[2c] The benefits of imprinted monolayers provide several advantages over bulk imprinted polymers such as excellent mass transfer of molecules into and out of imprinted sites.[3e,f] This is especially important for large templates such as proteins, which can be encapsulated and cannot be removed completely even from thin polymer matrices.[3e] Furthermore, rebinding of the templates is typically fast, and sensing can be further enhanced by the monolayer surfaces that facilitate transduction of binding signals detected in real time.[3e] Protein-imprinted monolayers from binary Langmuir monolayers containing positively charged lipids or glycolipids at the air−water interface have been constructed with the horizontal Langmuir−Blodgett (LB) technique by us and collaborators.[4] However, there are questions about the practical application of LB films because of their long-term stability.

Self-assembled monolayers (SAMs) through chemisorptions of surface-active molecules at a liquid−solid interface can directly build stable sensor platforms and modify physical or chemical properties of surfaces.[5] Crooks and co-worker[6] were the first to describe the concept of imprinted SAMs composed of nanoporous molecular assemblies. The imprinted SAMs on gold-coated chips using preadsorption[7] or preimmobilization[8] of small-template molecules followed by covalent attachment of alkanethiols were built, but the methods are unsuitable for protein imprinting because of unavailable specific binding sites except for hydrophobic imprinted cavities/monolayer surfaces for hydrophobic interactions. Rafailovich and co-workers[9] built protein-imprinted SAMs by mixing hydroxyl-terminated alkanethiols and template proteins in a solution of water and acetic acid followed by coadsorption of thiols and proteins on gold-coated chips. The hydrophobic interactions still played a dominant role. However, no progress on molecular imprinting with SAMs for protein recognition has been made since then.

Herein, we designed a disulfide molecule containing an oligoethylene glycol (OEG) terminal group and two amide groups (DHAP) (synthesis procedures are in the Supporting Information [SI]). OEG terminal moieties are known to be able to resist nonspecific protein binding,[10] and the amide groups incorporated in the chains not only can function on protein binding sites but also can strengthen the interactions between neighboring DHAP molecules for development of imprinted cavities. The strategy of a protein-imprinted SAM is illustrated in Figure 1. Template proteins, DHAP, and water-soluble functional thiols, such as glutathione (GSH, pI 5.93), mercaptoethylamine (MEA), or thioglycolic acid (TGA), were mixed in a water−acetic acid solution, and supramolecular

Received: March 8, 2013
Published: June 12, 2013

dx.doi.org/10.1021/ja402423r | J. Am. Chem. Soc. 2013, 135, 9248−9251

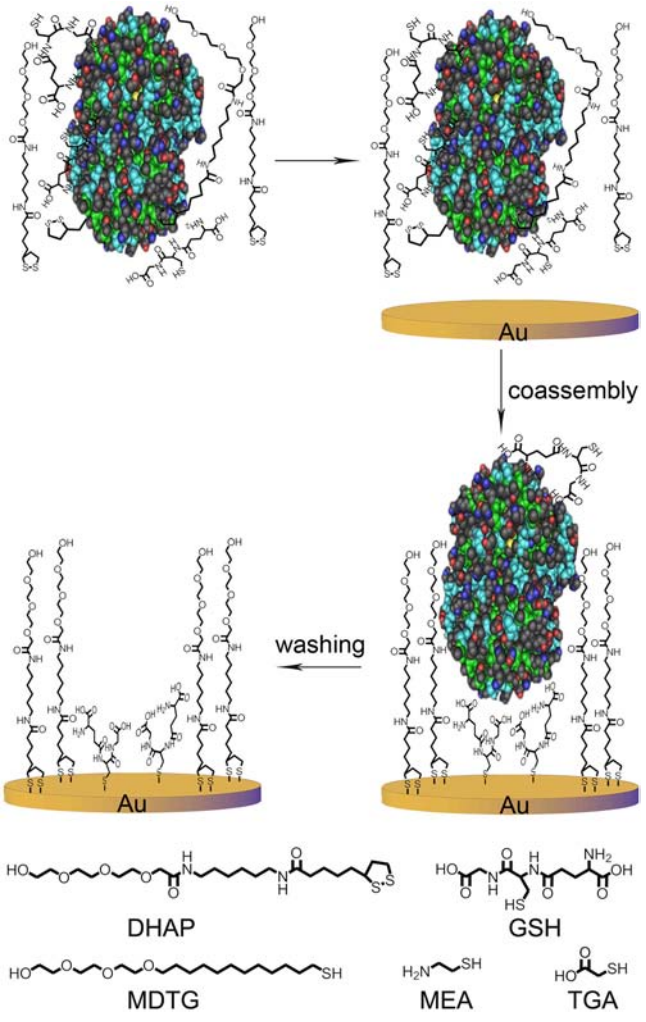

Figure 1. Preparation of a protein-imprinted SAM on a gold electrode (not drawn to scale) and chemical structures of relevant thiols.

structures of the proteins with DHAP and functional thiols were developed through hydrogen bonds and electrostatic interactions (Figures S1 and S2 in SI, NMR and saturation transfer difference (STD) NMR spectra). A gold-coated chip was then immersed for coassembly of DHAP and functional thiols together with the proteins through multiple interactions. Free DHAP in the solution preferentially bound to surrounding unoccupied zones of bound proteins on the chip surface for the development of imprinted cavities relative to the functional thiols, but could not displace the immobilized functional thiols interacting with the proteins through multiple binding sites. The protein-imprinted binary SAMs with multiple binding sites and biocompatible imprinted cavities were created after desorption of the template proteins together with removal of unimmobilized DHAP and functional thiols. The imprinted SAMs exhibited the ability to recognize target proteins with excellent sensitivity and selectivity.

Bovine hemoglobin (BHb, pI 7.0, $5.0 \times 5.5 \times 6.5$ nm^3)[11] and DHAP were dissolved in 10 mM phosphate buffer without NaCl (PB, pH 7.4) and acetic acid, respectively. BHb, DHAP, and GSH solutions (DHAP:GSH molar ratio of 40) were put into a small test tube and mixed homogenously. In this compromising dissolving process, a good solubility was available for DHAP, and the concentration of DHAP was about 0.1 mM, which was enough to form a stable SAM.[12] The molar ratio of BHb to DHAP was far less than 0.1, which could avoid protein aggregation.[9] A cleaned gold disk electrode was dipped into the solution mixture for 2.5 h to build a protein-imprinted SAM. Imprinted sites and cavities complementary to the template proteins were created in the SAM after removal of the templates with 1 M NaCl.[13] The differential pulse voltammograms (DPVs) of the BHb-imprinted SAM showed that reduction peak current of electroactive probe Fe-$(CN)_6^{4-/3-}$ significantly increased and then reached a constant value after 21 h of elution (Figure S3a in SI). This indicated the highly concentrated NaCl solution could efficiently remove the templates from the protein-imprinted SAM, while a small amount of proteins was only desorbed when washing with double-distilled water (Figure S3b in SI). The cyclic voltammograms (CVs) of the imprinted SAM exhibited typical redox peaks of $Fe(CN)_6^{4-/3-}$ after template removal (Figure 2A).

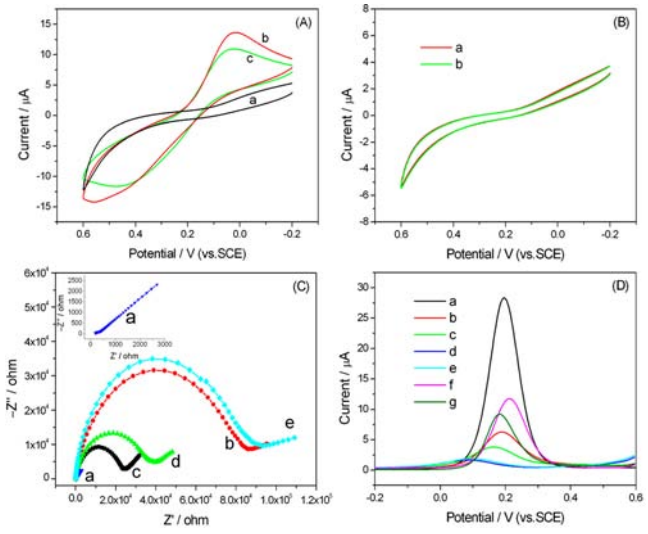

Figure 2. (A) CVs of the imprinted electrode (a) before and (b) after washing and (c) upon addition of BHb (24 μg/mL): scan rate, 0.1 V/s. (B) CVs of the nonimprinted electrode (a) before and (b) after addition of BHb (24 μg/mL); scan rate, 0.1 V/s. (C) EIS of different electrodes: (a) bare gold electrode; (b) imprinted electrode before BHb removal; (c) imprinted electrode after BHb removal; (d) imprinted electrode upon addition of BHb (24 μg/mL); (e) nonimprinted electrode. The frequency range was between 0.01 and 100000 Hz with the signal amplitude of 5 mV. (Inset) EIS of the bare gold electrode. (D) DPVs of different electrodes: (a) bare gold electrode; (b) imprinted electrode after BHb removal; (c) imprinted electrode upon addition of BHb (24 μg/mL); (d) nonimprinted electrode; (e) DHAP-modified electrode; (f) GSH-modified electrode; (g) imprinted electrode from BHb and DHAP after BHb removal. All of the electrodes were measured in 10 mM PB (pH 7.4) containing 2.5 mM $Fe(CN)_6^{4-/3-}$ and 0.1 M KCl.

The nonimprinted SAM (Figure 2B), which was prepared exactly like the imprinted one but without protein and formed only from DHAP and GSH, did not exhibit any electrochemical signal. These behaviors indicate that imprinted cavities were created in the imprinted SAM. Upon addition of BHb, the redox currents of the imprinted electrode decreased, which indicated BHb binding to the complementary sites and cavities in the imprinted SAM, and the CVs of the nonimprinted electrode remained unchanged.

Electrochemical impedance spectroscopy (EIS) was used to test the performance of the imprinted SAM. The semicircle

dx.doi.org/10.1021/ja402423r | J. Am. Chem. Soc. 2013, 135, 9248−9251

diameter corresponds to the electron transfer resistance, R_{et}. This resistance controls the electron transfer kinetics of the redox probes at the electrode interface (Figure 2C). A bare gold electrode exhibited an almost straight line, characteristic of a mass diffusion-limited electron transfer process. R_{et} was remarkably increased after the BHb-imprinted SAM was created on the electrode but significantly decreased after protein removal, whereas an increase in R_{et} was observed upon binding of BHb. However, the nonimprinted counterpart showed a maximum R_{et}. These results are consistent with those of the CV measurements.

Compared with the bare gold electrode, the imprinted SAM displayed a significant decrease in differential pulse voltammetry (DPV) of the reduction peak current (Figure 2D). In the presence of BHb, the peak current was further diminished because of protein binding to the imprinted sites and cavities. The nonimprinted electrode showed the minimal peak current, very comparable to that of the DHAP-modified electrode, which indicates that the nonimprinted SAM was nearly constituted by DHAP. This is because DHAP preferentially bound to the gold electrode to form a stable SAM, considering the large difference in molecular structure between DHAP and GSH. Moreover, the GSH-modified electrode showed a larger peak current than the imprinted SAM. It is confirmed that the imprinted SAM was constituted by DHAP and GSH with the imprinted cavities, which was different from the nonimprinted one. In addition, a control SAM imprinted only from BHb and DHAP without GSH was also prepared for comparison. The control imprinted one without GSH displayed a larger peak current than the imprinted SAM with GSH. This indicates that GSH was involved in the formation of both multiple binding sites and biocompatible imprinted cavities in the imprinted SAM to prevent direct contact of BHb with the gold electrode to a great extent.

To prove the role of the amide groups of DHAP in the imprinted sites and cavities, the electrochemical responses of the BHb-imprinted SAMs before and after protein removal were compared. A significant increase in reduction peak current was observed for the imprinted SAM prepared from BHb, GSH, and DHAP, while a small increase occurred for the imprinted SAM from BHb, GSH, and MDTG (amide-free in the chain) (Figure S4 in SI). It is mostly likely that BHb could not be easily removed from the protein-imprinted SAM due to the hydrophobic interactions between the proteins and MDTG hydrocarbon chains and that denaturation of proteins might be induced by the hydrophobic interactions. This verifies that the amide groups of DHAP were involved in the formation of hydrogen-bonded binding sites and biocompatible imprinted cavities.

The DPV peak current of the imprinted SAM decreased upon addition of BHb with increasing concentration (Figure S5 in SI). Electrochemical response was defined as a change in reduction peak current before and after protein binding (Δi). Δi increased with the increase of BHb concentration and then gradually approached a constant value up to about 100 μg/mL (Figure S6a in SI). However, very subtle changes in peak current were only observed for the nonimprinted electrode in the range of protein concentrations, which were very similar to those for the DHAP-modified electrode. Accordingly, the imprinted SAMs prepared from BHb, DHAP, and other functional thiols (MEA or TGA) and the corresponding nonimprinted ones showed similar electrochemical response behaviors (Figure S6b,c in SI). These results indicate that the target proteins could be recognized by the imprinted SAMs with complementary binding sites and cavities. The recognition of BHb by the imprinted SAM was further studied using surface-enhanced resonance Raman scattering (SERRS). BHb binding to the imprinted SAM followed by spreading of silver nanoparticles (AgNPs) (Figure S7 in SI) modified with 2-(iminodiacetic acid)ethanethiol in the presence of Cu^{2+} was subjected to SERRS (Figure S8 in SI).

To prove recognition specificity of the BHb-imprinted SAMs, myoglobin (Mb, pI 7.0, 2.5 × 3.5 × 4.5 nm^3),[14] ovalbumin (Ova, pI 4.6, 7.0 × 4.5 × 5.0 nm^3),[15] and lysozyme (Lyz, pI 11.0, 3.0 × 3.0 × 4.5 nm^3)[16] were chosen for comparison. These proteins have large differences in isoelectric point and dimension. The imprinted SAMs showed a very sensitive response to the original template BHb but were almost insensitive to nontemplate proteins (Mb, Ova, and Lyz) (Figure 3A). Mb and Lyz have smaller dimensions than BHb

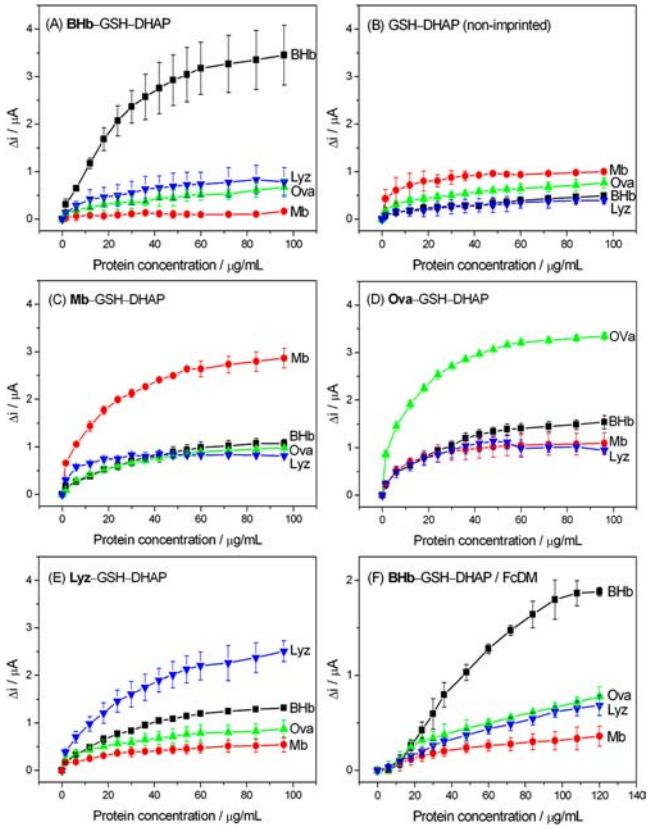

Figure 3. Decrease of DPV reduction peak current of the imprinted electrodes (template protein, GSH, and DHAP) in 10 mM PB (pH 7.4) containing 2.5 mM $Fe(CN)_6^{4-/3-}$ and 0.1 M KCl as a function of concentration of different proteins: (A) BHb; (B) no template (nonimprinted); (C) Mb; (D) Ova; (E) Lyz; (F) BHb with FcDM as a probe (2.5 mM). The error bars represent standard deviations for triplicate tests.

and could enter the imprinted cavities, and Ova has dimensions comparable to those of BHb with a slight difference and could enter the imprinted cavities at a right orientation mode. However, the nontemplate proteins could not be efficiently recognized or captured by the imprinted SAMs, similar to the nonimprinted counterparts in the presence of these proteins (Figure 3B). These results unambiguously demonstrate that there were binding sites on the surfaces of the imprinted SAMs

dx.doi.org/10.1021/ja402423r | J. Am. Chem. Soc. 2013, 135, 9248−9251

that specifically recognized the template protein. When Mb, Ova and Lyz were respectively imprinted, similar recognition selectivity was observed dependent on the template protein (Figure 3C−E). In order to avoid possible influence of the charge on the proteins on accessibility of electroactive probes to imprinted cavities, the noncharged probe ferrocene dimethanol (FcDM) was used for further identification of protein recognition specificity (Figure S9 in SI and Figure 3F). Similarly, the BHb-imprinted SAMs exhibited recognition selectivity of BHb in comparison with nontemplate proteins.

The number of imprinted sites[6b] on the surfaces of the BHb-imprinted SAMs were estimated to be 5.5×10^7 imprinted sites/cm^2 with the probe $Fe(CN)_6^{4-/3-}$ and 8.6×10^7 imprinted sites/cm^2 with the probe FcDM from the corresponding CVs (Figure 2A and Figure S10 in SI), respectively. Accordingly, the numbers of imprinted sites/cm^2[6b] for the SAMs imprinted with the templates Mb, Ova, and Lyz were respectively estimated to be 1.4×10^8, 7.2×10^7, and 3.5×10^7 in the case of FcDM. The fractional surface coverages of sites imprinted with the templates BHb, Mb, Ova, and Lyz[6a] were further estimated to be 2.1×10^{-5}, 1.6×10^{-5}, 1.6×10^{-5}, and 3.0×10^{-6}, respectively.

For the BHb-imprinted SAMs with the functional thiols MEA and TGA (Figure S11 in SI) and the Ova-imprinted SAM with MEA (Figure S12 in SI), the differences in binding affinities between the template and nontemplate proteins confirm that both multiple interactions and geometrical complementarity were required for specific protein binding to the imprinted SAMs considering the isoelectric points and dimensions of these proteins and the functional thiols used. These results demonstrate that the created protein-imprinted SAMs possessed excellent ability to bind specific target proteins determined by multiple binding sites and imprinted cavities. The proposed strategy has universal significance in creation of protein-imprinted SAMs for binding specific proteins.

As the proof of concept, the protein-imprinted SAMs were created with multiple binding sites and biocompatible imprinted cavities from functional thiols and DHAP containing OEG terminal moieties and two amide groups incorporated in the chain in the water−acetic acid solution. DHAP played an important role in the formation of multiple binding sites and biocompatible cavities in addition to resisting nonspecific protein binding. The created protein-imprinted SAMs exhibited excellent ability to bind specific target proteins determined by multiple binding sites and imprinted cavities. The sensitive and label-free detection of target proteins offers an ideal candidate for artificial biological materials for biosensors based on biomolecular recognition. The strategy generates tailor-made monolayer surfaces with specific protein binding and opens the possibility of controlled assembly of intellectual biomaterials and preparation of biosensors.

■ ASSOCIATED CONTENT

Supporting Information

Synthesis details, experimental details, and supporting figures and illustrations. This material is available free of charge via the Internet at http://pubs.acs.org.

■ AUTHOR INFORMATION

Corresponding Author

xzdu@nju.edu.cn

Notes

The authors declare no competing financial interest.

■ ACKNOWLEDGMENTS

This work was supported by National Natural Science Foundation of China (No. 21273112) and Natural Science Foundation of Jiangsu Province (BK2012719). We thank Dr. Xiaoliang Yang at Nanjing University for her tests of 600 MHz NMR spectra.

■ REFERENCES

(1) (a) Wulff, G. *Angew. Chem., Int. Ed.* **1995**, *34*, 1812−1832. (b) Vlatakis, G.; Andersson, L. I.; Müller, R.; Mosbach, K. *Nature* **1993**, *361*, 645−647.

(2) (a) Wulff, G. *Chem. Rev.* **2002**, *102*, 1−27. (b) Wulff, G.; Liu, J. *Acc. Chem. Res.* **2012**, *45*, 239−247. (c) Bossi, A.; Bonini, F.; Turner, A. P. F.; Piletsky, S. A. *Biosens. Bioelectron.* **2007**, *22*, 1131−1137.

(3) (a) Shi, H.; Tsai, W.-B.; Garrison, M. D.; Ferrari, S.; Ratner, B. D. *Nature* **1999**, *398*, 593−597. (b) Hansen, D. E. *Biomaterials* **2007**, *28*, 4178−4191. (c) Dhruv, H.; Pepalla, R.; Taveras, M.; Britt, D. W. *Biothechnol. Prog.* **2006**, *22*, 150−155. (d) Kim, E.; Kim, H.-C.; Lee, S. G.; Lee, S. J.; Go, T.-J.; Baek, C. S.; Jeong, S. W. *Chem. Commun.* **2011**, *47*, 11900−11902. (e) Balamurugan, S.; Spivak, D. A. *J. Mol. Recognit.* **2011**, *24*, 915−929. (f) Turner, N. W.; Jeans, C. W.; Brain, K. R.; Allender, C. J.; Hlady, V.; Britt, D. W. *Biotechnol. Prog.* **2006**, *22*, 1474−1489.

(4) (a) Du, X.; Hlady, V.; Britt, D. *Biosens. Bioelectron.* **2005**, *20*, 2053−2060. (b) Du, X.; Wang, Y. *J. Phys. Chem. B* **2007**, *111*, 2347−2356. (c) Du, X.; Wang, Y.; Ding, Y.; Guo, R. *Langmuir* **2007**, *23*, 8142−8149. (d) Turner, N. W.; Wrigh, B. E.; Hlady, V.; Britt, D. W. *J. Colloid Interface Sci.* **2007**, *308*, 71−80. (e) Zheng, H.; Du, X. *J. Phys. Chem. B* **2009**, *113*, 11330−11377. (f) Zheng, H.; Du, X. *Biochim. Biophys. Acta* **2011**, *1808*, 2128−2135. (g) Zheng, H.; Du, X. *Biochim. Biophys. Acta* **2013**, *1828*, 792−800.

(5) (a) He, X.-P.; Wang, X.-W.; Jin, X.-P.; Zhou, H.; Shi, X.-X.; Chen, G.-R.; Long, Y.-T. *J. Am. Chem. Soc.* **2011**, *133*, 3649−3657. (b) Mack, E. T.; Snyder, P. W.; Perez-Castillejos, R.; Whitesides, G. M. *J. Am. Chem. Soc.* **2011**, *133*, 11701−11715.

(6) (a) Chailapakul, O.; Crooks, R. M. *Langmuir* **1993**, *9*, 884−888. (b) Chailapakul, O.; Crooks, R. M. *Langmuir* **1995**, *11*, 1329−1340.

(7) (a) Li, X.; Husson, S. M. *Langmuir* **2006**, *22*, 9658−9663. (b) Bi, X.; Yang, K.-L. *Anal. Chem.* **2009**, *87*, 527−531.

(8) (a) Doron, A.; Portnoy, M.; Lion-Dagan, M.; Katz, E.; Willner, I. *J. Am. Chem. Soc.* **1996**, *118*, 8937−8944. (b) Lahav, M.; Katz, E.; Doron, A.; Patolsky, F.; Willner, I. *J. Am. Chem. Soc.* **1999**, *121*, 862−863. (c) Lahav, M.; Katz, E.; Willner, I. *Langmuir* **2001**, *17*, 7387−7395.

(9) Wang, Y. T.; Zhou, Y. X.; Sokolov, J.; Rigas, B.; Levon, K.; Rafailovich, M. *Biosens. Bioelectron.* **2008**, *24*, 162−166.

(10) (a) Prime, K. L.; Whitesides, G. M. *J. Am. Chem. Soc.* **1993**, *115*, 10714−10721. (b) Herrwerth, S.; Eck, W.; Reinhardt, S.; Grunze, M. *J. Am. Chem. Soc.* **2003**, *125*, 9359−9366.

(11) Perutz, M. F.; Muirhead, H.; Cox, J. M.; Goaman, L. C. G.; Mathews, F. S.; McGandy, E. L.; Webb, L. E. *Nature* **1968**, *219*, 29−32.

(12) Porter, M. D.; Bright, T. B.; Allara, D. L.; Chidsey, C. E. D. *J. Am. Chem. Soc.* **1987**, *109*, 3559−3568.

(13) Fu, G. Q.; He, H. Y.; Chai, Z. H.; Chen, H. C.; Kong, J.; Wang, Y.; Jiang, Y. Z. *Anal. Chem.* **2011**, *83*, 1431−1436.

(14) Kendrew, J. C.; Dickerson, R. E.; Strandberg, B. E.; Hart, R. G.; Davies, D. R.; Phillips, D. C.; Shore, V. C. *Nature* **1960**, *185*, 422−427.

(15) Stein, P. E.; Leslie, A. G. W.; Finch, J. T.; Turnell, W. G.; McLaughlin, P. J.; Carrell, R. W. *Nature* **1990**, *347*, 99−102.

(16) Blake, C. C. F.; Koenig, D. F.; Mair, G. A.; North, A. C. T.; Phillips, D. C.; Sarma, V. R. *Nature* **1965**, *206*, 757−761.